

SPECTROSCOPIC ORBITS OF THREE DWARF BARIUM STARS

By *P. L. North*¹, *A. Jorissen*², *A. Escorza*^{2,3}, *B. Miszalski*^{4,5}, and *J. Mikoajewska*⁶

¹*Institute of Physics, Laboratory of Astrophysics,*

Ecole Polytechnique Fédérale de Lausanne (EPFL), Switzerland

²*Institut d'Astronomie et d'Astrophysique, Université Libre de Bruxelles, Belgium*

³*Instituut voor Sterrenkunde, KU Leuven, Belgium*

⁴*South African Astronomical Observatory*

⁵*Southern African Large Telescope Foundation*

⁶*N. Copernicus Astronomical Center, Polish Academy of Sciences, Warsaw, Poland*

Barium stars are thought to result from binary evolution in systems wide enough to allow the more massive component to reach the asymptotic giant branch and eventually become a CO white dwarf. While Ba stars were initially known only among giant or subgiant stars, some were subsequently discovered also on the main sequence (and known as dwarf Ba stars). We provide here the orbital parameters of three dwarf Ba stars, completing the sample of 27 orbits published recently by Escorza *et al.* with these three southern targets. We show that these new orbital parameters are consistent with those of other dwarf Ba stars.

Introduction

Barium stars are not evolved enough to synthesize in their interiors and dredge up to their surface the s-process elements (including Ba) that are very abundant in their atmospheres. On the other hand, we have convincing statistical indications that they all belong to SB1-type binary systems [1] [2], and UV observations have revealed the white dwarf nature of the companion of some of them [3] [4] [5]. This leads to the following scenario – that has become common wisdom – to explain their overabundance of s-process elements: the initially more massive component evolved into an asymptotic giant branch (AGB) star, synthesized and dredged up carbon and s-process elements, expelled its envelope, part of which was accreted by the "innocent bystander", namely the initially secondary component, and the latter thereby became the Ba star we observe today while the other component cooled to a white dwarf. The mass ratio underwent a reversal in the process. The mass transfer may occur through wind, (wind) Roche lobe overthrow or common

envelope evolution [6]; the details are still debated, but the net result is a long orbital period (a few hundred days to several decades) and a small eccentricity [2] [7].

Interestingly, Ba stars were known initially only among G- and K-type giants (they were dubbed Ba giants when belonging to Population I, and CH giants when belonging to Population II) [8] [9] and subgiants (dubbed CH subgiants) [10], though some of the latter are actually dwarfs [11]. The existence of main sequence Ba stars was fully recognized only in the early 1990's [12] [13] [14] [15] [16] [17] [18], among F- and G-type stars. The question then arose as to whether giant Ba stars might be the descendants of Ba dwarfs. Even though the latter appear on average less massive than the former [7], this is the result of a selection bias (dwarf Ba stars are difficult to detect among the more massive main-sequence A and late-B stars). From a dynamical viewpoint, the two families appear similar, as revealed by their almost perfect overlap* in the eccentricity – period diagram (Fig. 1).

Ba dwarfs and subgiants are interesting because their mass determination is easier than for Ba giants. Therefore if a relative astrometric orbit is accessible in addition to the spectroscopic one, the mass of the companion can be determined. If only the spectroscopic orbit is known, but for a large enough sample of Ba systems, a statistical estimate of the companion mass can be obtained assuming random orbit orientations. This was done by e.g. North *et al.* [18] and by Escorza *et al.* [7], and resulted in a companion mass close to $0.6 M_{\odot}$, as expected for a white dwarf. The first sample consisted of 14 orbits, while the second sample included 27 orbits.

In this work, we present the orbital parameters of three more Ba stars, namely HD 202400, HD 222349, and HD 224621. The elemental abundances of the first two were determined by North *et al.* [16] [17] and by Luck & Bond [19] for the third. All three can be considered as belonging to the main sequence, even though HD 224621 had been classified as a "CH subgiant", because their surface gravities determined through high-resolution spectroscopy are $\log g > 3.7$.

Sample and observations

The stars HD 202400 and HD 222349 had been classified as F2 Ba 1 and G2 Ba 1 respectively by Lü *et al.* [20] and were studied with high-dispersion spectroscopy by North *et al.* [16]. HD 224621 was first classified as a subgiant CH star by Bond [10], then studied with high-dispersion spectroscopy by Luck & Bond [19]. Table 1 lists the stellar parameters adopted by these authors and shows that they indeed belong to the main sequence. The magnitudes, colour indices and *Gaia* DR2 parallaxes are also listed. The spectral classification and photometry were taken from the *Simbad* database. All three stars populate the southern sky, with declinations $\delta < -36^{\circ}$. The masses listed in Table 1 were derived as in ref. [7].

*The three dwarf Ba stars with $P > 2000$ d seemingly falling in the "low-eccentricity gap" ($P > 1000$ d, $e \leq 0.05$) of the eccentricity – period diagram (Fig. 1) have error bars on the eccentricity compatible with them lying just at the boundary of the gap.

Table 1

Basic properties of the sample stars. The stellar parameters are those adopted by North *et al.* [16] and by Luck & Bond [19], except for the mass (see text). The B and V magnitudes are taken from the Simbad database, and the parallaxes from the Gaia DR2.

Star	Sp. type	V	$B - V$	π	T_{eff}	$\log g$	[Fe/H]	M	
HD	Other id.			[mas]	[K]	[cgs]	[dex]	[M_{\odot}]	
202400	HIP 105294	Ap Sr	9.18	0.39	5.92	6200	4.0	−0.7	0.98
			±0.01	±0.02	±0.07	±100	±0.2	±0.1	±0.08
222349	SAO 247972	G5/K0+A/F(Sr)	9.22	0.48	8.16	6000	3.8	−0.9	0.73
			±0.01	±0.02	±0.10	±100	±0.2	±0.1	±0.05
224621	HIP 118266	G0III/IV	9.55	0.63	12.60	6000	4.0	−0.4	0.90
			±0.02	±0.03	±0.30	±200	±0.3	±0.1	±0.06

The radial-velocity (RV) observations were carried out mainly with the *Coravel* spectrovelocimeter [21] attached to the 1.54-m Danish telescope at ESO-La Silla (Chile). For HD 202400 and HD 222349, recent observations were carried out with the 11-m *Southern African Large Telescope (SALT* [22] [23]) using the *High Resolution Spectrograph (HRS* [24] [25] [26]) in the medium resolution (MR) mode, providing resolving powers $R = 43\,000$ and $R = 40\,000$ for the blue and red arms respectively. The basic data products [27] were reduced with the MIDAS pipeline developed by Kniazev *et al.* [28] which is based on the ECHELLE [29] and FEROS [30] packages. Heliocentric corrections were applied to the data using VELSET of the RVSAO package [31]. While the *Coravel* radial velocities are obtained at the hardware level by a physical cross-correlation between the observed spectrum and a mask based on the spectrum of Arcturus, the *HRS* velocities are obtained *a posteriori* by a digital cross-correlation between the observed spectrum and F0 or G2 masks [7]. These two stars were also observed once each with the *Coralie* spectrograph attached to the Swiss 1.2-m telescope at ESO-La Silla, and their radial velocities obtained as well by cross-correlation with an appropriate mask. A few RV measurements (five for HD 202400, five for HD 222349, and one for HD 224621) are based on spectra taken with the *CES* spectrograph attached to the 1.4-m *Coud Auxiliary Telescope (CAT)* at ESO-La Silla with a resolving power $R = 60\,000$. The RV values are averages over a few lines fitted by Gaussians, and their adopted errors are the rms dispersion of the RVs given by the individual lines. A single RV estimate for HD 202400 is based on the positions of the Mg I $\lambda 5172$, $\lambda 5183$ lines of the Mg I triplet and of the two lines of the Na I D doublet, measured on a spectrum taken with the *FEROS* instrument attached to the 1.52-m telescope at ESO-La Silla. The radial velocities are listed in Table 2.

Results

The search for the most probable orbital period and the determination of the orbital parameters were made using the DACE software, that is publicly available (<https://dace.unige.ch>) and is optimized for the search of exoplanets but also appropriate for the analysis of binary stars. The analysis is made in three

Table 2 Measured radial velocities for the sample stars. Columns 3 and 7 indicate the instrument used.

Star	HJD	Instr. or	RV	σ_{RV}	HJD	Instr.	RV	σ_{RV}
HD	-2400000	ref.	[km s ⁻¹]	[km s ⁻¹]	-2400000		[km s ⁻¹]	[km s ⁻¹]
202400	47831.533	CES	-24.53	2.0	50705.654	Coravel	-27.64	3.66
	47833.579	CES	-27.72	1.52	51320.925	Coralie	-15.40	1.0
	47834.572	CES	-26.94	1.97	51449.636	FEROS	-16.10	1.44
	48765.938	Coravel	-22.10	2.8	58026.336	HRS	-18.38	0.92
	49235.658	CES	-27.09	0.56	58051.258	HRS	-17.86	0.73
	49237.584	CES	-26.36	1.76	58061.290	HRS	-18.04	1.23
	49522.860	Coravel	-24.67	2.30	58064.262	HRS	-17.89	1.11
	49526.858	Coravel	-21.43	2.42	58238.651	HRS	-12.92	0.67
	49613.607	Coravel	-24.24	3.16	58292.501	HRS	-12.80	0.74
	49880.838	Coravel	-12.39	1.76	58329.501	HRS	-12.80	0.75
	50083.534	Coravel	-17.05	2.99	58361.458	HRS	-14.87	1.66
	50274.821	Coravel	-25.62	2.27	58413.347	HRS	-16.49	0.60
	50410.513	Coravel	-27.21	2.98				
222349	47830.618	CES	39.28	0.54	50083.528	Coravel	32.30	0.40
	48842.873	Coravel	30.36	0.34	50276.941	Coravel	35.61	0.42
	48887.707	CES	30.09	0.27	50410.529	Coravel	36.91	0.39
	49234.652	CES	27.28	0.41	50705.751	Coravel	39.88	0.44
	49236.648	CES	27.43	0.58	51320.935	Coralie	38.73	0.09
	49237.665	CES	27.20	0.41	58084.343	HRS	28.24	0.15
	49522.947	Coravel	27.55	0.42	58097.304	HRS	27.86	0.16
	49610.759	Coravel	28.16	0.43	58355.587	HRS	25.39	0.12
	49880.923	Coravel	30.72	0.42	58409.275	HRS	26.42	0.03
	224621	43054.791	LB91	14.0	0.5	47400.747	Coravel	7.82
45544.942		Coravel	9.11	0.40	47514.549	Coravel	13.20	0.32
45979.627		Coravel	14.67	0.34	47756.814	Coravel	6.53	0.35
46274.842		Coravel	12.22	0.37	47783.732	Coravel	7.37	0.33
46338.704		Coravel	21.77	0.34	48055.927	Coravel	5.78	0.35
46395.566		Coravel	20.21	0.34	48074.928	Coravel	6.03	0.35
46399.535		Coravel	19.12	0.34	48160.791	Coravel	18.42	0.33
46632.880		Coravel	20.19	0.36	48463.862	Coravel	17.00	0.31
46667.773		Coravel	22.20	0.32	48842.861	Coravel	21.81	0.32
46687.751		Coravel	20.85	0.33	48872.783	Coravel	18.37	0.35
46692.706		Coravel	20.97	0.39	49235.747	CES	10.26	0.38
46724.637		Coravel	17.06	0.32	49522.898	Coravel	13.11	0.36
46728.617		Coravel	16.26	0.30	49610.765	Coravel	5.87	0.34
47043.744		Coravel	15.64	0.33	49880.926	Coravel	6.97	0.40
47049.782		Coravel	14.08	0.35	50083.546	Coravel	19.95	0.37
47069.667		Coravel	11.30	0.35	50276.937	Coravel	11.84	0.36
47100.598		Coravel	7.17	0.33	50410.535	Coravel	18.91	0.36
47104.615		Coravel	7.20	0.35	50706.750	Coravel	21.01	0.39
47370.933		Coravel	12.41	0.38	50795.536	Coravel	6.66	0.49

steps: the first consists in a periodogram, on which the user can select the most probable period; the second is a first keplerian fit of the orbital parameters, following the method described by Delisle *et al.* [32]; the third and final step consists in a Monte-Carlo Markov Chain (MCMC) that determines final values and realistic errors for the orbital parameters, as described by Daz *et al.* [33], [34]. The MCMC even allows us to adjust possible RV zero-point offsets between different instruments. We have determined the orbital parameters both using this possibility and under the assumption of negligible offsets; in general the former option remains unsatisfactory in that it artificially lowers the reduced chi-square, so we rather adopted the latter option. The resulting orbital parameters are displayed in Table 3. The RV curves are shown in Figs. 2, 3, and 4.

Table 3

Orbital parameters of the sample stars obtained using the DACE code, including the MCMC. The errors quoted correspond to 1σ , i.e. to the 68.27% confidence interval.

Star HD	P_{orb} [d]	e	T_p [HJD -2400000]	ω [$^\circ$]	K_1 [km s^{-1}]	γ [km s^{-1}]	$f(m)$ [M_\odot]	$a_1 \sin i$ [AU]	σ_{res} [km s^{-1}]	N
202400	1396.6 ± 7.3	0.222 ± 0.067	48523 ± 133	14 ± 33	7.26 ± 0.46	-21.56 ± 0.42	0.0513 ± 0.0100	0.906 ± 0.055	0.89	25
222349	3018.6 ± 5.6	0.112 ± 0.023	54964 ± 45	123.9 ± 5.7	6.89 ± 0.11	33.657 ± 0.076	0.1004 ± 0.0048	1.899 ± 0.033	0.268	18
224621	308.092 ± 0.094	0.023 ± 0.011	48172.6 ± 15.5	316.8 ± 18.2	8.173 ± 0.092	13.822 ± 0.060	0.01741 ± 0.00059	0.2314 ± 0.0026	0.376	38

Discussion

Adding these three new orbits to the 27 published by Escorza *et al.* [7], the number of orbits for systems hosting dwarf or subgiant Ba stars now amounts to 30. However, one of the systems studied by Escorza *et al.* is an SB2 system (HD 114520) and could actually be a triple system, if one accepts the prevailing paradigm about the formation of Ba stars as a given; the WD would then follow a much wider orbit, the period of which remains to be determined. Another system, HD 48565, is clearly triple but, as it is an SB1, it is not possible to know whether the WD belongs to the inner or to the outer system. Thus we are left with 28 binary systems whose statistical properties may be investigated.

In Fig. 1, we presented the sample $e - P$ diagram which revealed an almost perfect coincidence between the locations of the two samples, suggesting that giant Ba stars (and their cooler analogues – the extrinsic S stars) are indeed the descendants of the dwarf Ba stars. Using the BINSTAR evolution code [35], this hypothesis will be further evaluated in a paper in preparation (Escorza *et al.* 2020).

In Fig. 5 we show the relation between the mass of the Ba star and its metallicity [Fe/H] for both giant (filled circles) and dwarf (open squares) Ba stars. Here, the triple system HD 48565 is included, because

the orbital elements do not matter, and one can be confident that the non-degenerate, non-Ba component is faint enough that neither the mass nor the metallicity of the primary component is biased; the diagram thus includes 29 dwarf Ba stars (open squares). The giant Ba stars are taken from Fig. 17 of Jorissen *et al.* [2]. For the reason mentioned in the introduction (dwarf Ba stars are difficult to detect among the more massive main-sequence A and late-B stars), dwarf Ba stars so far appear to be restricted to a narrower mass range than are giant Ba stars. Low-mass Ba stars (with $M < 2 M_{\odot}$) cover a large metallicity range ($-1 \leq [\text{Fe}/\text{H}] \leq 0$), whereas the most massive (giant) Ba stars ($M \geq 4 M_{\odot}$), being relatively young, are restricted to high metallicities ($-0.2 \leq [\text{Fe}/\text{H}]$).

It seems appropriate here to dig a bit deeper into the question as to why no dwarf Ba star is known with a mass larger than about $1.6 M_{\odot}$. A selection bias undoubtedly does occur, due to the fast rotation of most intermediate-mass stars on the main sequence, that broadens the spectral lines and thus makes abundance determinations difficult. However, some A-type stars are slow rotators, therefore some of them could in principle be detected as Ba stars. Indeed Ba has been found overabundant in several of these (*e.g.*, by Lemke [36], and Takeda *et al.* [37]), but many of them are classified as Am stars (see, *e.g.*, Fig. 1 of Çay *et al.* [38] for the elemental abundances in two typical Am stars), and most Am stars are short-period binary systems, with a period distribution that is not compatible with that of Ba stars. Ba is overabundant in many chemically-peculiar stars, from those of the HgMn type (among the late B-type stars, see, *e.g.*, Monier *et al.* [39]), to those of the SrCrEu type (among the mid A-type stars, see, *e.g.*, Guthrie [40], Cowley [41], and Kochukov *et al.* [42]). The problem is that such stars also show underabundance of carbon, contrary to both dwarf and giant Ba stars, and their abundance anomalies are thought to be due to radiative diffusion rather than mass-transfer in a binary system (see refs. [43] and [44]). Especially telling is the case of the magnetic Ap star HR 3831, where the Ba overabundance may reach a factor as large as 10^5 in some places of the stellar surface, according to abundance Doppler imaging [42]: such high overabundances cannot be explained by the mass-transfer scenario invoked for Ba stars. Furthermore, the high efficiency of radiative diffusion in slowly rotating intermediate-mass stars suggests that any abundance anomaly due to mass-transfer in a binary system will be quickly superseded and erased by the radiative diffusion mechanism, making the identification of such systems all the more problematic. Interestingly, the possible link between Am stars and barium stars had already been proposed by Hakkila [45], though his discussion about how to reconcile the discrepant period distributions remains unconvincing.

Related questions are whether Sirius is a Ba star or not, and why Procyon does not show Ba overabundance. The first question has been addressed by Landstreet [46]: Sirius does show a significant (1.4 dex) Ba overabundance and it does have a white dwarf companion, but it is classified as a mild Am star (A0mA1 Va, according to Gray *et al.* [47]) and indeed has abundances typical of Am stars. Its orbit has a long period (50.13 yr) and a rather large eccentricity (0.591), but such figures are still within the orbital parameters

covered by Ba stars (see Fig. 1). For instance, HD 119185 [2] has $P_{\text{orb}} = 60$ yr and $e = 0.6$. It is highly probable that radiative diffusion has been and is still being at work in Sirius A, but precisely because of this, it remains impossible to know how much processed material it has accreted from its former AGB companion. Sirius A has a mass $M = 2.06 M_{\odot}$, so it is perfectly representative of those stars that are massive enough to have almost no convective zone, thus permitting radiative diffusion to take place. On the other hand, the WD has a mass $M = 1.02 M_{\odot}$, corresponding to an initial stellar mass $M \sim 5 M_{\odot}$ according to the semi-empirical initial-final mass relation of Cummings *et al.* [48]. Such high-mass AGB stars with solar metallicity are unable to yield substantial quantities of s-process elements [49], suggesting that radiative diffusion alone is responsible for the Ba overabundance of Sirius A. Procyon A has a mass $M = 1.5 M_{\odot}$ that is similar to that of dwarf Ba stars. It also has a white dwarf companion, with $M = 0.60 M_{\odot}$, on an orbit with $P_{\text{orb}} = 40.82$ yr and $e = 0.407$, quite compatible with some orbits of Ba stars. However, its Ba abundance, although slightly enhanced, remains solar within 1σ (and other heavy s-process elements like Nd and Sm are 2σ below solar) according to Kato & Sadakane [50]. Why, then, is Procyon A not a Ba star? Although this seems to contradict the mass-transfer scenario at first sight, at least two factors may reconcile this scenario with the lack of Ba overabundance: (i) the anti-correlation between the overabundance of s-process elements and the orbital period, and (ii) the anti-correlation between that overabundance and $[\text{Fe}/\text{H}]$ (see ref. [2]), and the solar metallicity of Procyon.

Acknowledgements

PN thanks Dr. Maxime Marmier for digging into the old *Coravel database*, thereby providing us with precious RV values obtained with the southern *Coravel* scanner attached to the 1.54-m Danish telescope at ESO La Silla, Chile. PN also thanks the colleagues who contributed to this observational effort, especially Mr. Bernard Pernier of Geneva Observatory and Dr. Jean-Claude Mermilliod of Institut d’astronomie de l’Universit de Lausanne. Some RVs were obtained using the *Coralie* spectrograph attached to the Swiss 1.2-m *Euler* telescope at ESO La Silla Observatory, Chile, while others were obtained using the *CES* spectrograph attached to the *CAT* 1.4-m telescope at ESO La Silla. One measurement was made with the *FEROS* spectrograph attached to the 1.5-m ESO telescope at ESO La Silla. Recent measurements were gathered with the *Southern African Large Telescope (SALT)* using the *HRS* within the *SALT* programme 2017-1-MLT-010 (PI. B. Miszalski). This research has been partly funded by the National Science Centre, Poland, through grant OPUS 2017/27/B/ST9/01940 to JM. Polish participation in *SALT* is funded by grant No. MNiSW DIR/WK/2016/07. Keplerian model initial conditions are computed using the formalism described in Delisle *et al.* [32], while the MCMC algorithm is described in Daz *et al.* [33], [34]. The orbital parameters and their errors were obtained using the DACE code. PN also thanks Dr. Damien Segransan for his help in using the DACE software. This research has been partly funded by the Belgian Science Policy Office under contract BR/143/A2/STARLAB. AE acknowledges support from the Fonds voor Wetenschappelijk Onder-

zoek Vlaanderen (FWO) under contract ZKD1501-00-W01. BM acknowledges support from the National Research Foundation (NRF) of South Africa. This research has made use of the *Simbad* database, operated at CDS, Strasbourg, France.

References

- (1) R. D. McClure & A. W. Woodsworth, *ApJ*, **352**, 709, 1990.
- (2) A. Jorissen *et al.*, *A&A*, **626**, A127, 2019
- (3) E. Böhm-Vitense *et al.*, *ApJ*, **278**, 726, 1984.
- (4) E. Böhm-Vitense *et al.*, *ApJ*, **533**, 969, 2000.
- (5) R. O. Gray *et al.*, *AJ*, **141**, 160, 2011.
- (6) M. I. Saladino *et al.*, *A&A*, 626, A68, 2019.
- (7) A. Escorza *et al.*, *A&A*, **626**, A128, 2019.
- (8) W. P. Bidelman & P. C. Keenan, *ApJ*, **114**, 473, 1951
- (9) P. C. Keenan, *ApJ*, **96**, 101, 1942
- (10) H. E. Bond, *ApJ*, **194**, 95, 1974
- (11) A. Escorza *et al.*, *A&A*, **608**, A100, 2017
- (12) P. North & A. Duquennoy, *A&A*, **244**, 335, 1991
- (13) P. North & T. Lanz, *A&A*, **251**, 489, 1991
- (14) A. Jorissen & H. M. J. Boffin, in A. Duquennoy & M. Mayor (eds.), *Binaries as tracers of star formation*, (Cambridge Univ. Press), p. 110, 1992.
- (15) P. North, in A. Duquennoy & M. Mayor (eds.), *Binaries as tracers of star formation*, (Cambridge Univ. Press), p. 202, 1992.
- (16) P. North *et al.*, *A&A*, **281**, 775, 1994
- (17) P. North *et al.*, *A&A*, **292**, 350, 1994
- (18) P. North *et al.*, in R. F. Wing (ed.), *The carbon star phenomenon*, IAU Symp 177, p. 269, 2000.
- (19) R. E. Luck & H. E. Bond, *ApJS*, **77**, 515, 1991.
- (20) P. K. Lü *et al.*, *ApJS*, **52**, 169, 1983.

- (21) A. Baranne *et al.*, *Vistas in Astronomy*, **23**, 279, 1979.
- (22) D. A. H. Buckley *et al.*, in Proc. SPIE Vol. 6267, *Society of Photo-Optical Instrumentation Engineers (SPIE) Conferences Series*, **62670Z**, 2006.
- (23) D. O'Donoghue *et al.*, *MNRAS*, **372**, 151, 2006.
- (24) D. G. Bramall *et al.*, in Proc. SPIE Vol. 7735, *Society of Photo-Optical Instrumentation Engineers (SPIE) Conferences Series*, **77354F**, 2010.
- (25) D. G. Bramall *et al.*, in Proc. SPIE Vol. 8446, *Society of Photo-Optical Instrumentation Engineers (SPIE) Conferences Series*, **84460A**, 2012.
- (26) L. A. Crause *et al.*, in Proc. SPIE Vol. 9147, *Society of Photo-Optical Instrumentation Engineers (SPIE) Conferences Series*, **91476T**, 2014.
- (27) S. M. Crawford *et al.*, in Proc. SPIE Vol. 7737, *Society of Photo-Optical Instrumentation Engineers (SPIE) Conferences Series*, **773725**, 2010.
- (28) A. Y. Kniazev *et al.*, *MNRAS*, **459**, 3068, 2016.
- (29) P. Ballester, in European Southern Observatory Conference and Workshop Proceedings, Vol. 41, eds. P. J. Grosbøl & R. C. E. de Ruijscher, p. 177, 1992.
- (30) O. Stahl *et al.*, in Astronomical Society of the Pacific Conference Series, Vol. 188, *Optical and Infrared Spectroscopy of Circumstellar Matter*, eds. E. Guenther, B. Stecklum, & S. Klose, p. 331, 1999.
- (31) M. J. Kurtz & D. J. Mink, *PASP*, **110**, 934, 1998.
- (32) J.-B. Delisle *et al.*, *A&A*, **590**, A134, 2016.
- (33) R. F. Daz *et al.*, *MNRAS*, **441**, 983, 2014.
- (34) R. F. Daz *et al.*, *A&A*, **585**, A134, 2016.
- (35) P. Davis *et al.*, *A&A*, **556**, A4, 2013.
- (36) M. Lemke, *A&A*, **240**, 331, 1990.
- (37) Y. Takeda, *Journal of the Korean Astronomical Society*, **41**, 83, 2008.
- (38) I. H. Çay *et al.*, *PASP*, **128**, 054201, 2016.
- (39) R. Monier *et al.*, *Ap&SS*, **361**, 139M, 2016.
- (40) B. N. G. Guthrie, *Ap&SS*, **3**, 542, 1969.

- (41) C. R. Cowley, *ApJS*, **32**, 631, 1976.
- (42) O. Kochukhov *et al.*, *A&A*, **424**, 935, 2004.
- (43) G. Michaud, *ApJ*, **160**, 641, 1970.
- (44) J. Borsenberger *et al.*, *A&A*, **139**, 147, 1984.
- (45) J. Hakkila, *AJ*, **98**, 699, 1989.
- (46) J. D. Landstreet, *A&A*, **528**, A132, 2011.
- (47) R. O. Gray *et al.*, *AJ*, **126**, 2048, 2003.
- (48) J. D. Cummings, *ApJ*, **871**, L18, 2019.
- (49) A. I. Karakas & M. Lugaro, *ApJ*, **825**, 26, 2016.
- (50) K. Kato & K. Sadakane, *A&A*, **113**, 135, 1982.

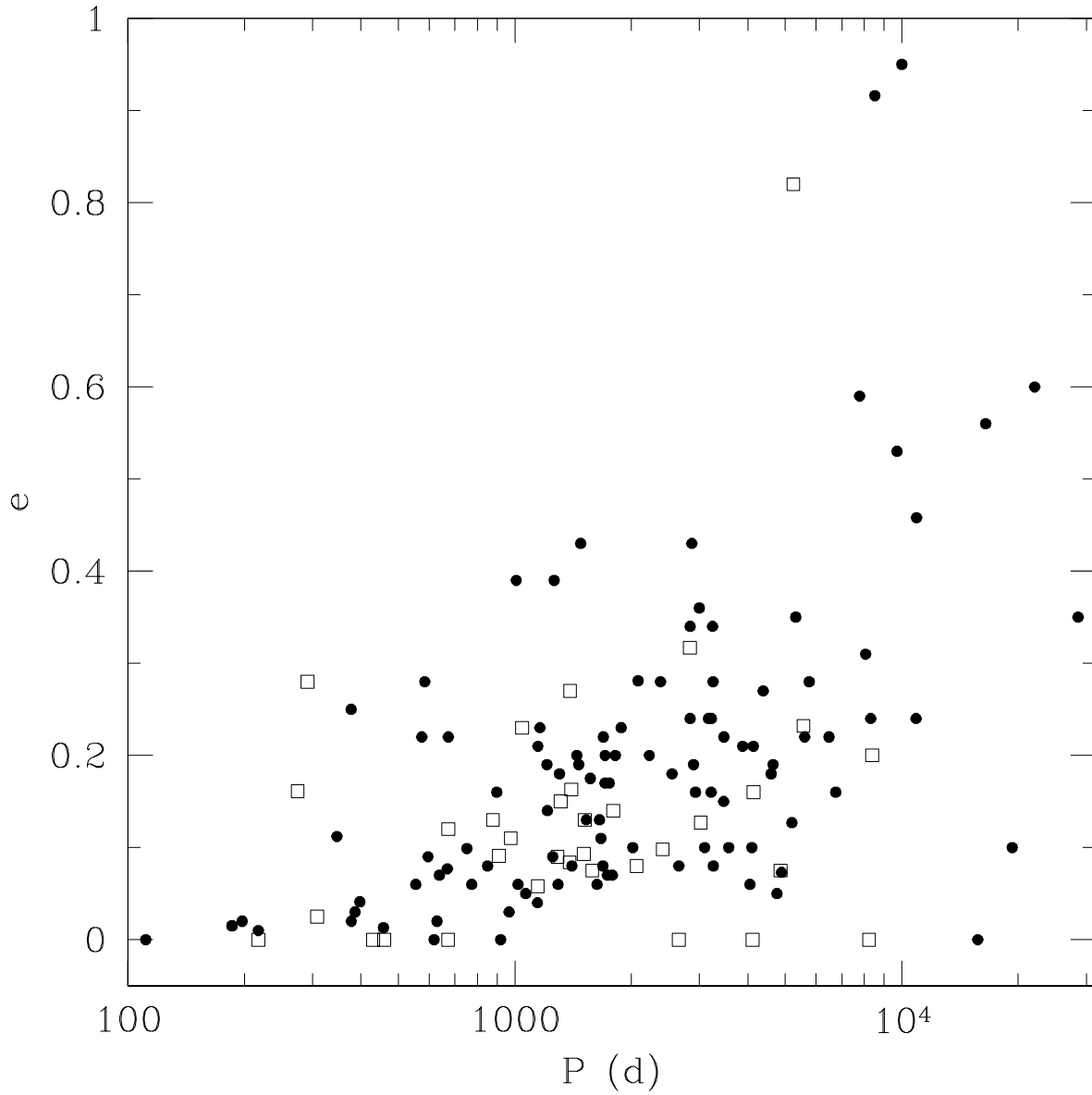


FIG. 1

The $e - P$ diagram for dwarf Ba and subgiant CH stars (open squares; from ref. [7] and the present work) and giant Ba and S stars (filled circles; [2]).

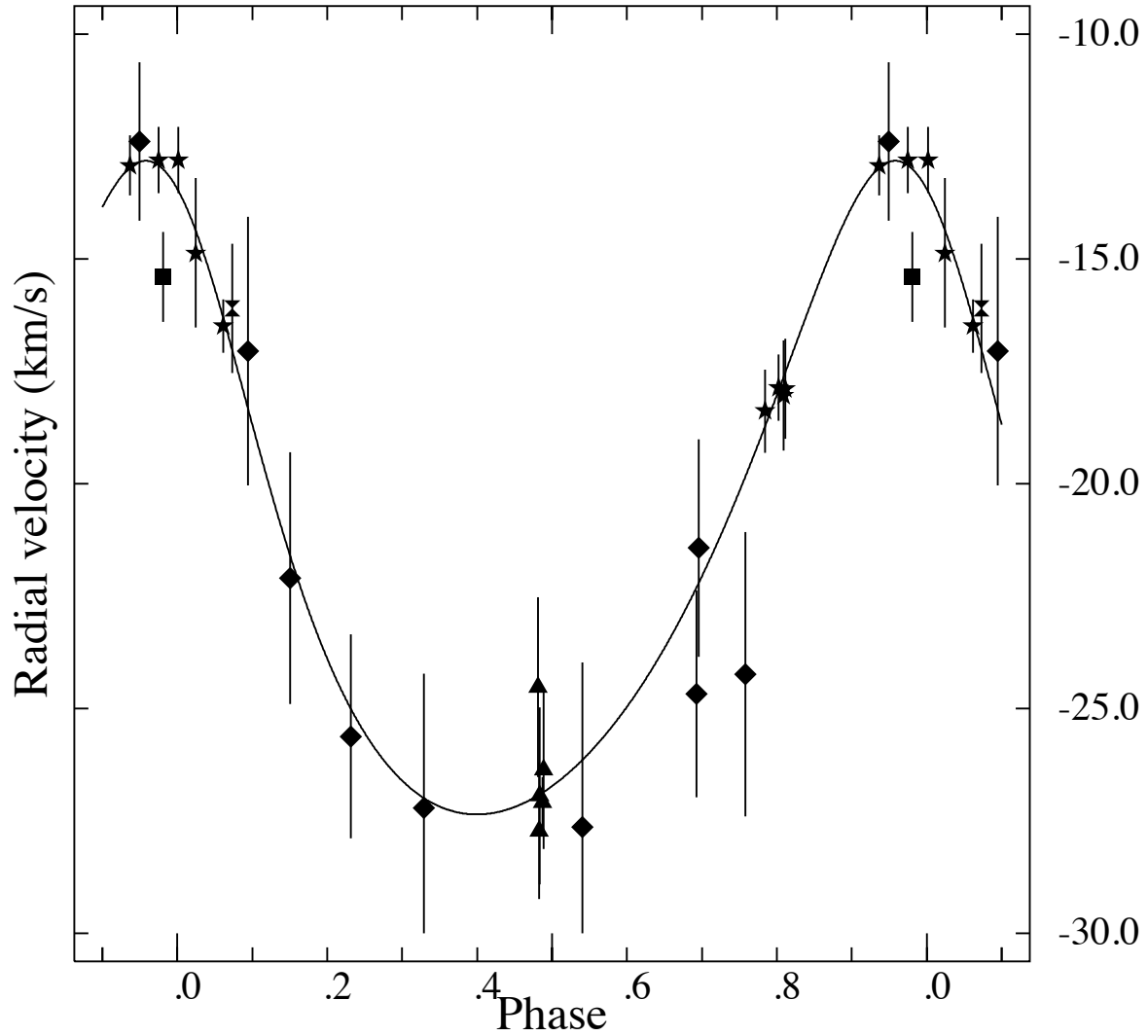


FIG. 2

Radial velocities (RV) of HD 202400 as a function of orbital phase. Symbols are as follows: triangles (*CAT*), hourglass (*FEROS*), stars (*SALT*), square (*Coralie*), lozenges (*Coravel*). The large RV errors and dispersion around the fitted curve are due to a relatively high projected rotational velocity.

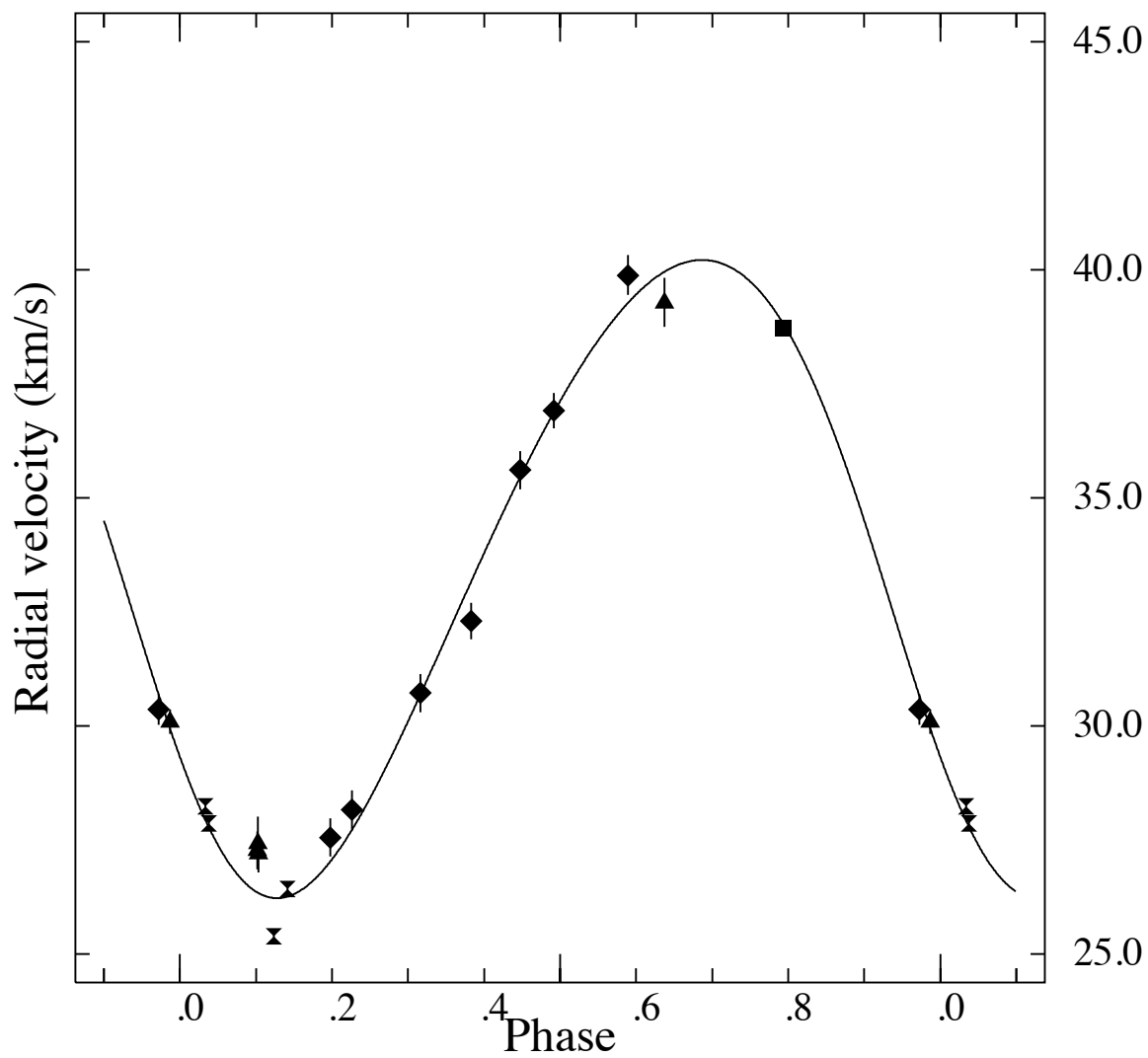


FIG. 3

Same as Fig. 2, but for HD 222349. Symbols are as follows: triangles (*CAT*), hourglasses (*SALT*), square (*Coralie*), lozenges (*Coravel*).

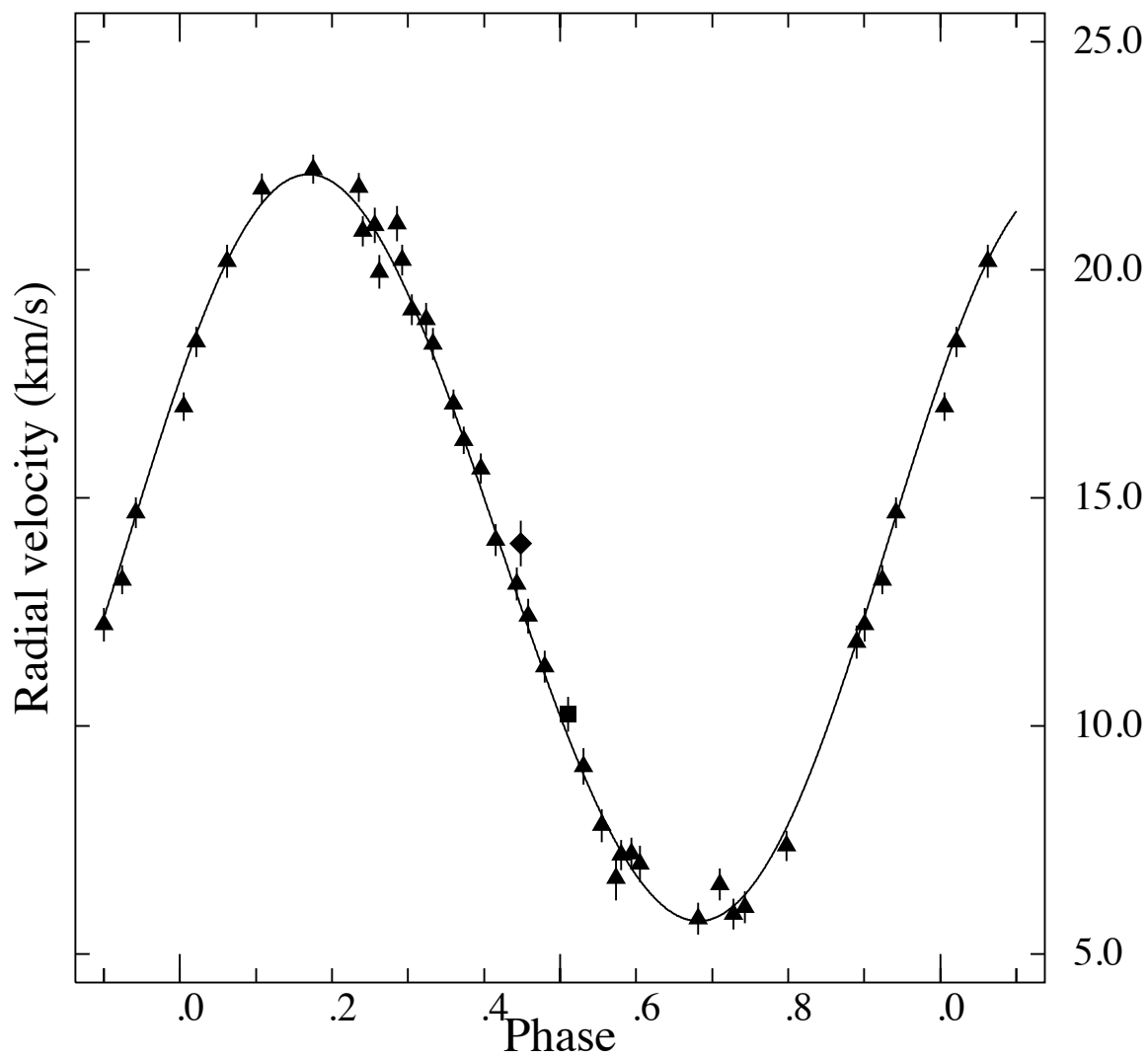


FIG. 4

Same as Fig. 2, but for HD 224621. Symbols are as follows: triangles (*Coravel*), square (*CAT*), lozenge (ref. [19]).

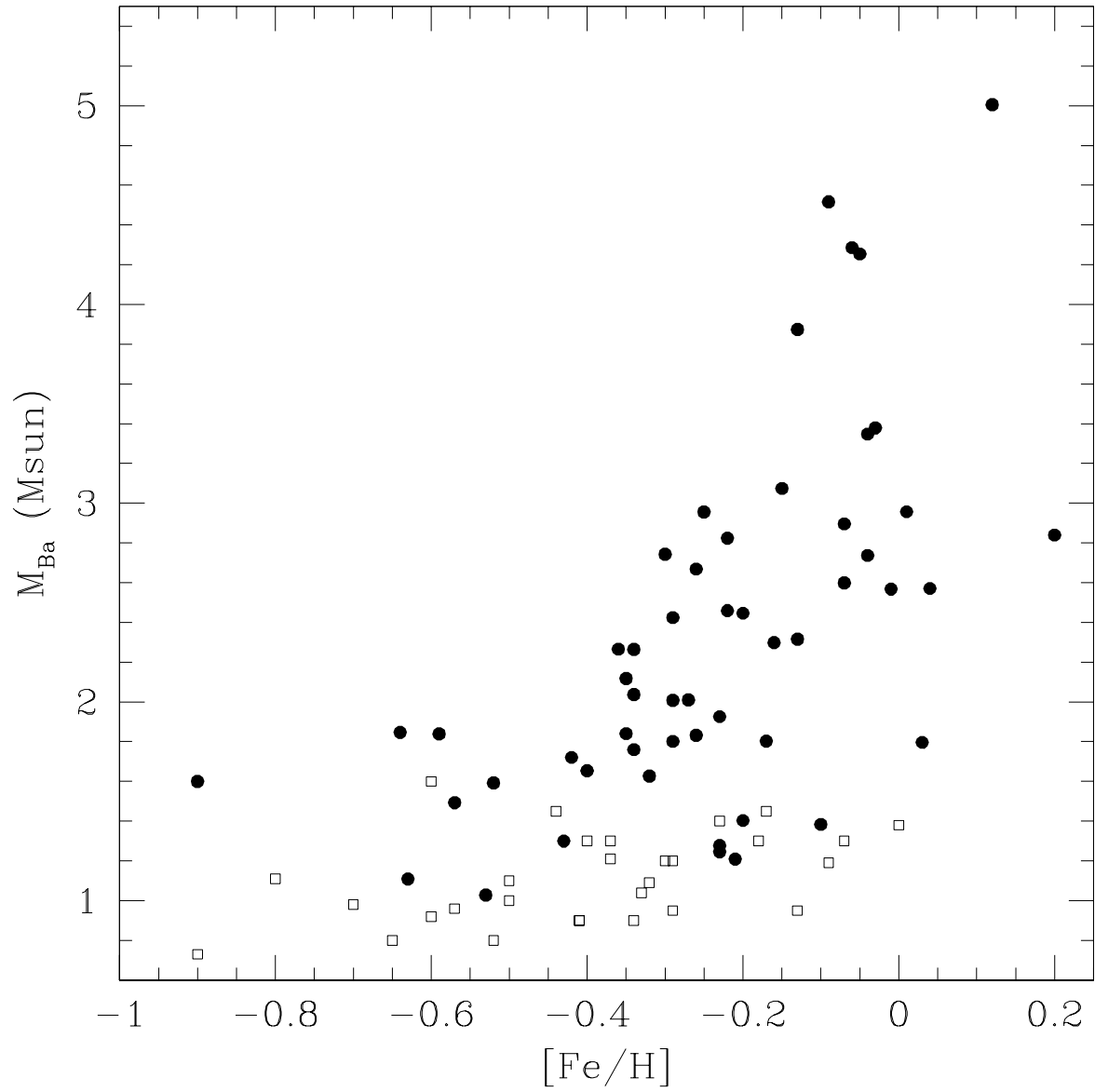


FIG. 5
 Barium star mass vs. $[\text{Fe}/\text{H}]$, for barium giants (filled circles (ref. [2])) and barium dwarfs (open squares, from this work and ref. [7]).